Article ID:1004-4213(2010)02-0233-5

Modeling of the Radiation Impedance Characteristics for Photoconductive Antenna*

XU Ying[1], CHEN Hai-bin[1], HONG Zhi[2,†]
(1 *Center for Optical and Electromagnetic Research, Zhejiang University, Hangzhou* 310058, *China*)
(2 *Center for Terahertz Research, China Jiliang University, Hangzhou* 310018, *China*)

Abstract: To overcome the disadvantage of low radiation power for photoconductive antenna, three types of antennas, including dipole, bow-tie and spiral antennas, are studied, where finite integration technology are used to compute their radiation impedances. The simulation results show that the impedance of dipole antenna is dependent on the dipole length, width, photoconductive gap and the width of transmission line, and has a peak value in resonant frequency, so the dipole antenna is suitable for applications working at specific terahertz frequency. The bow-tie and spiral antennas, known as broadband antennas, have approximately stable impedance over the terahertz frequency range under study. The simulation results also show that, the interdigitated fingers, which can be modelled as an additional capacitance, cause the antenna impedance to fall dramatically at high frequency.

Key words: Terahertz; Photomixing; Dipole antenna; Bow-tie antenna; Spiral antenna
CLCN: O431 **Document Code**: A **doi**: 10.3788/gzxb20103902.0233

0 Introduction

The terahertz (THz) region of the electromagnetic spectrum, typically considered to occupy 100 GHz to 10 THz, lies between microwave and infrared. Terahertz radiation can penetrate many materials with modest attenuation, and lots of chemical substances and explosive materials exhibit characteristic spectral responses at terahertz frequencies. Additionally, being at sub-millimeter wavelengths, it is of low energy and non-ionising. These unique properties make terahertz radiation a potentially powerful technique in the security screening[1-2], non-destructive testing[3], and medical imaging[4].

Photoconductive antennas, which can work at room temperature, are widely used in pulsed and continuous terahertz generation and detection[1,5-6]. As continuous-wave terahertz emitters, they are usually used as photomixers pumped by two light beams whose frequency difference is in the terahertz range. The output of terahertz beam has narrow linewidth, and wide range tunable properties, but the main restriction is their limited terahertz radiation power. The terahertz output power for photoconductive antenna is proportional to its radiation impedance according to photomixing principle[7-8]. Many researchers have performed optimization of antenna design to improve their radiation properties. Mclntosh, et al experimentally compared the output power from spiral antennas with different photoconductive gap areas[9]. Grogery, et al studied the terahertz emission from bow-tie antenna with bare gap and interdigitated fingers, and concluded that the terahertz output efficiency at high frequencies was additionally dependent on the design of photomixer fingers[10]. Theoretical methods were presented by Brown to evaluate the terahertz output power from photoconductive structures consisting of interdigitated electrodes[11]. The dependence of carrier lifetime and carrier velocity on the electric field was taken into account by Saeedkia, et al[12].

This paper systematically and theoretically studies three types of antennas with different mechanical designs, and compares their radiation impedances through simulation.

1 Photoconductive antennas

Three types of photoconductive antennas, including dipole antenna[8], bow-tie antenna[10,13] and spiral antenna[9,14], are studied in this paper. Fig. 1 shows the schematic diagrams of the three

* Supported by the National Natural Science Foundation of China (60576042)
† Tel: 0571-86845096 Email: hongzhi@cjlu.edu.cn
Received date: 2009-03-19 Revised date: 2009-05-07

kinds of photoconductive antennas. The dipole antenna with two designs of electrodes coupled to the external circuit is shown in Fig. 1(a), and an equivalent circuit, which is suitable for bow-tie and spiral antenna too, is given in Fig. 2.

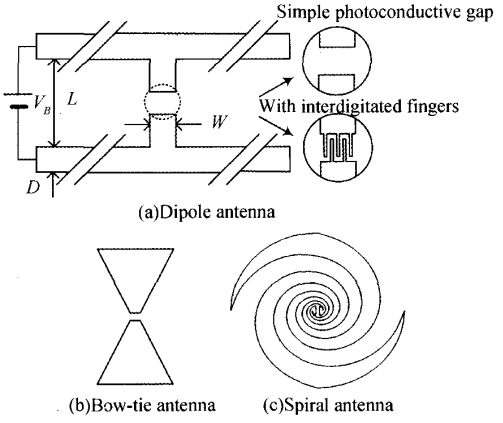

Fig. 1 Schematic diagrams of dipole antenna, bow-tie antenna and spiral antenna

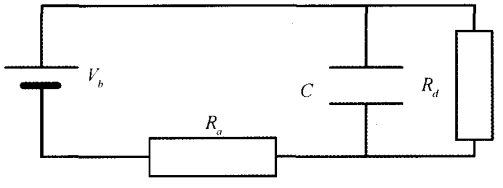

Fig. 2 Equivalent circuit for the biased photoconductive antenna

In the antenna design, there are two categories of photoconductive antennas, one with simple gap and the other with interdigitated fingers. In the former case, Ref [8] has demonstrated that the antenna length and width have effects on resonant frequency for dipole antenna. Photoconductive gap and transmission line width are the other main parameters for dipole antenna too. Bow-tie angle and turns of spiral affect the radiation properties for bow-tie antenna and spiral antenna, respectively.

Photomixing is a technique to generate continuous-wave terahertz radiation with photoconductive antennas. The procedure for photomixing proceeds as follows[11-12]. A bias photoconductive antenna fabricated on a semiconductor is illuminated with an optical beam. The optical beam generates free carriers in the photoconductive gap, when the photon energy of the optical beam is larger than the band gap of the semiconductor. If the carrier lifetime of the semiconductor is short enough under bias condition, it can respond to the current modulation in the photoconductive antenna. Terahertz radiation generates and is emitted into free space.

Continuous-wave terahertz emission occurs by illuminating the electrode gap with two single-mode continuous-wave laser beams, whose average power is P_1 and P_2, and angular frequency is ω_1 and ω_2, respectively. The instantaneous optical power incident on the antenna is given below [15]

$$P(w,t)=P_1+P_2+2\sqrt{mP_1P_2}\cos(\omega t+\varphi) \quad (1)$$

$$P_i=\int\left(cn\varepsilon_0\frac{E_i^2}{2}\right)\mathrm{d}S \quad (i=1,2,\omega=\omega_1-\omega_2) \quad (2)$$

where $P_i(i=1,2)$ are averaged powers of the two beams, c is the speed of light in vacuum, n is the refractive index of the media, ε_0 is the dielectric constant of vacuum, φ is the relative phase between the two optical beam, and m is the spatial-mixing efficiency of the two beams. The frequency difference of the two incident laser beams w can be tuned in the terahertz frequency range and the integration in equation (2) is carried out over the beam cross section.

The carrier density in the photoconductive gap is given by

$$\frac{\mathrm{d}n}{\mathrm{d}t}=\eta P(\omega,t)-\frac{n}{\tau} \quad (3)$$

where n is the photo-excited carrier number, η is the excitation efficiency, and τ is the photo-excited carrier lifetime.

Using the equivalent circuit diagram for the photoconductive antenna and the equation (3), the terahertz output power $P_{THz}(\omega)$ *is given by*

$$P_{THz}(\omega)=\frac{J_0^2R_a}{2[1+(\omega\tau)^2][1+(\omega R_aC)^2]} \quad (4)$$

where $J_0(=G_0V_b)$ is the DC photocurrent, G_0 is the time-averaged photoconductance for the average total incident power, V_b is the bias voltage, Ra is the radiation impedance of the antenna, and C is the capacitance of the photoconductive gap. $R_d=1/G$, where G is the photoconductance of the antenna.

Equation (4) shows that the terahertz output power is proportional to the radiation impedance of the antenna, and the square of DC conductance and bias voltage. Since the impedance of photoconductive antenna is important for continuous-wave terahertz radiation, the impedance characteristics of these above three types of photoconductive antennas are studied.

2 Simulation results

In the simulation, the impedances of different antennas are calculated numerically as a function of

frequency based on finite integration technique. The antenna geometries are firstly defined within a finite-element mesh and metal electrodes as perfect electrical conductors, and the terahertz radiation is modeled by generating a Gaussian terahertz wave in the photoconductive gap and examining the frequency-dependent current and voltage at the antenna feed. The antenna radiation impedance is calculated by monitoring the voltage and current within the antenna. Finally, the curves of impendence are plotted as a function of frequency.

Fig. 3 shows the results for dipole antennas with two different antenna lengths, where (a) is 40 μm and (b) is 80 μm. The parameters for dipole antennas in Fig. 3 are dipole length, dipole width, photoconductive gap and transmission line width. In Fig. 3, the Dipole Ⅰ 40/10/10/10 stands for a dipole antenna with dipole length 40 μm, dipole width 10 μm, photoconductive gap 10 μm and transmission line width 10 μm. The simulation results in 3 (a) and 3 (b) show fundamental resonant frequencies of about 0. 85 THz and 0. 76 THz, respectively, which have relatively high impedances of a few 1 000 Ω. Other weak resonant frequencies also exist when the dipole length becomes short enough. The resonant frequency moves towards higher frequency domain as the gap size becomes larger, where the resonant frequency for Dipole Ⅰ (0. 86 THz) is higher than Dipole Ⅲ (0. 84 THz). Moreover, the resonant impedance becomes smaller when the transmission line width becomes larger. It is shown from Fig. 3 that, the resonant frequency moves towards lower frequency domain when the dipole length becomes longer, which is consistent with the experimental results in ref [8]. However, even when the antenna length becomes very short, high resonant frequency can not be achieved[16]. The simulation results also show that the resonant frequency moves towards lower frequency domain as the dipole width becomes larger. The dipole antennas mentioned above are a kind of end-feed dipole antenna proposed by Gregory et al[16], the resonant frequency of which is inversely proportional to the dipole length. This conclusion is supported by the results of calculation.

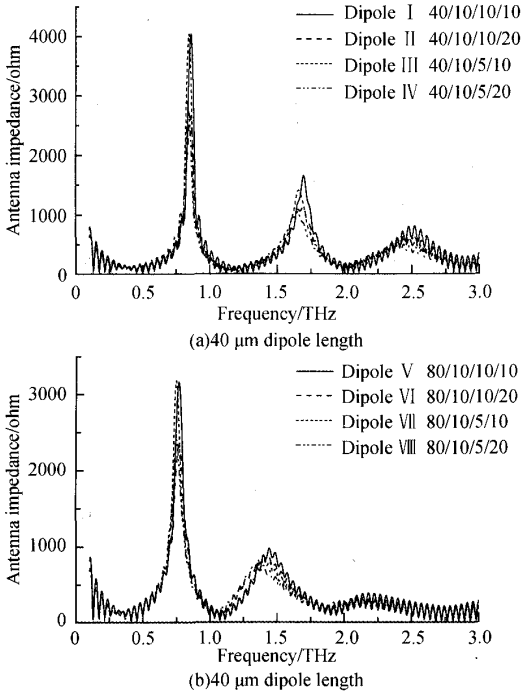

Fig. 3　Impedances of Dipole antennas

The parameters for bow-tie antenna are antenna length, bow-tie angle and photoconductive gap. It is shown in Fig. 4 that, the antenna impedance becomes lower as the bow-tie angle becomes larger, and the influence of photoconductive gap is evident at high frequency. Moreover, the bow-tie antenna has approximately stable impedance of about a few 100 Ω over the calculated frequency range.

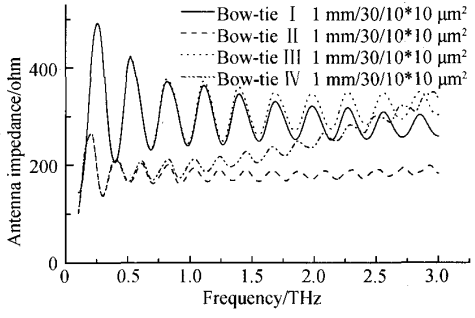

Fig. 4　Impedances of Bow-tie antennas

The spiral antennas under simulation is a kind of self-complimentary spiral with a constant impedance of 188. 5 Ω for a semiconductor half-space[14]. Fig. 5 shows the simulation results for Spiral antenna Ⅰ, Ⅱ, Ⅲ, Ⅳ. The parameters for spiral antenna are turns of spiral and photoconductive gap. It can be concluded that, the impedance in high frequency domain becomes higher as the photoconductive gap becomes larger. Meanwhile, the turns of spiral has little effect on the impedance when the other parameters are the same. Fig. 5 indicates that spiral antenna is also a type of broadband antenna.

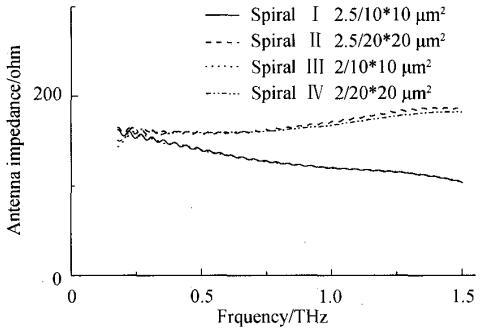

Fig. 5 Impedances of Spiral antennas

In the latter case of antenna design, the interdigitated fingers are modeled as a lumped capacitance in parallel with the photoconductive active area. Fig. 6 shows that the simulation results for three types of antennas with interdigitated fingers, the capacitances of which are about 1 fF[14] for the case of the active area of 100 μm^2, the electrode width of 0.5 μm and the width of the gap between the electrodes of 1.5 μm. Fig. 6(a) shows that fundamental resonant frequency still exist for the dipole antenna with interdigitated fingers, but the resonant frequency moves to lower and the radiation impedance decreases as the frequency goes up to 3 THz. For bow-tie antenna and spiral antenna, it can be seen in Fig. 6(b) and (c) that the additional capacitance of interdigitated fingers causes the antenna impedance to fall dramatically at frequency beyond 0.5 THz, which has been presented experimentally by Gregory and Brown et al. that the capacitive effect makes the radiation impedance fall apparently as the frequency increases[10,14].

The above simulations results show that, the dipole antenna has the property of high impedance, no less than a few thousand ohms around the fundamental resonant frequency, while the bow-tie and spiral antenna have stable impedance about a few hundred ohms over the calculated frequency range. As the terahertz radiant power is proportional to the antenna impedance, the magnitude of the resonant power for dipole antenna increases by up to an order of magnitude at the specific frequency, compared with broadband antennas such as bow-tie antenna and spiral antenna. In fact, remarkable improvement of terahertz output power has been achieved with high-impedance antenna designs as dual-dipole and dual-slot antennas[17].

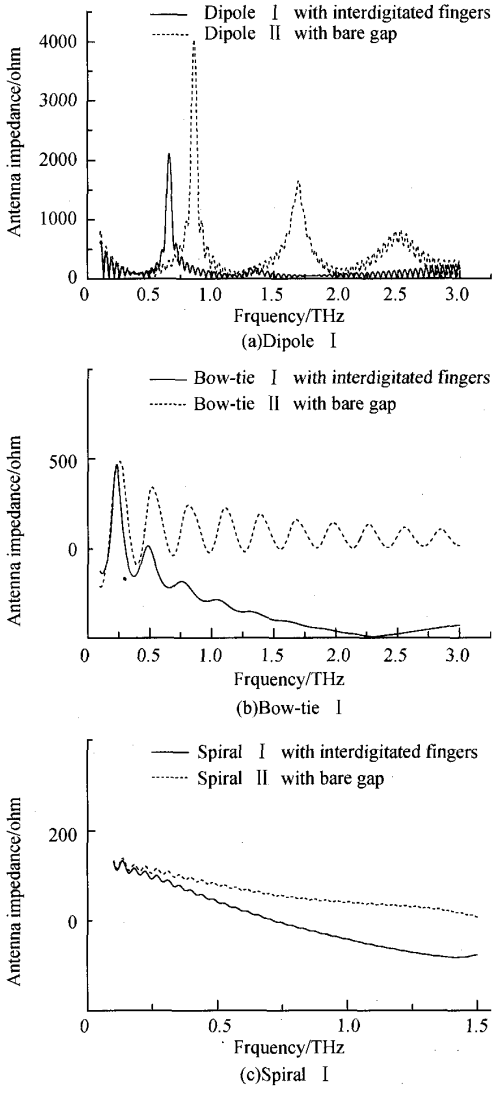

Fig. 6 Impedances of three kinds of antennas with and without interdigitated fingers

3 Conclusions

In summary, we have studied the impedance properties of three types of photoconductive antennas for continuous terahertz radiation. The results show that dipole antenna, as a kind of resonant antenna, has high radiation impedance around the resonant frequency, which can result in efficient terahertz radiation at some specific frequency. The bow-tie and spiral antennas are more suitable for broadband terahertz applications, because they have stable impedance over a quite broad frequency range. Moreover, the interdigitated fingers have effect on the three types of antennas at high frequencies. All the above antennas will be experimentally studied in our continuous-wave terahertz system in future.

References

[1] GREGORY I S, TRIBE W R, BAKER C, *et al*. Continuous-wave terahertz system with a 60 dB dynamic range [J]. *Appl Phys Lett*, 2005, **86**(20): 204104.

[2] XI Zai-jun, XIAO Ti-qiao, ZHANG Zeng-yan, *et al*. Investigation on two-dimensional transmission imaging with terahertz wave by time domain spectroscopy [J]. *Acta Photonica Sinica*, 2006, **35**(8): 1171-1174.

[3] MITTLEMAN D M, JACOBSEN R H, NUSS M C. T-ray imaging [J]. *IEEE J Selected Topics in Quantum Electronics*, 1996, **2**(3): 679-692.

[4] NAKAJIMA S, HOSHINA H, Yamashita M, *et al*. Terahertz imaging diagnostics of cancer tissues with a chemometrics technique [J]. *Appl Phys Lett*, 2007, **90**(4): 041102.

[5] JIA Wan-li, JI Wei-li, SHI Wei. Two-dimensional Monte Carlo simulation of screening of the bias field in terahertz generation from semi_insulated GaAs photoconductors [J]. *Acta Physica Sinica*, 2007, **56**(4): 2042-2046.

[6] LIU Ming-li, ZHANG Tong-yi, SUN Chuan-dong, *et al*. Characterization of high-power narrow-band terahertz radiation generation using large-aperture photoconductive antennas [J]. *Acta Photonica Sinica*, 2007, **36**(10): 1793-1798.

[7] TANI M, GU P, HYODO M, *et al*. Generation of coherent terahertz radiation by photomixing of dual-mode lasers [J]. *Opt Quantum Electron*, 2000, **32**(4): 503-520.

[8] MATSUURA S, TANI M, SAKAI K. Generation of coherent terahertz radiation by photomixing in dipole photoconductive antennas [J]. *Appl Phys Lett*, 1997, **70**(3): 559-561.

[9] MCINTOSH K A, BROWN E R, NICHOLS K B, *et al*. Terahertz photomixing with diode lasers in low-temperature-grown GaAs [J]. *Appl Phys Lett*, 1995, **67**(26): 3844-3846.

[10] GREGORY I S, BAKER C, TRIBE W R, *et al*. Optimization of photomixers and antennas for continuous-wave terahertz emission [J]. *IEEE J Quantum Electron*, 2005, **41**(5): 717-728.

[11] BROWN E R. A photoconductive model for superior GaAs THz photomixers [J]. *Appl Phys Lett*, 1999, **75**(6): 769-771.

[12] SAEEDKIA D, SAFAVI-NAEINI S. A comprehensive model for photomixing in ultrafast photoconductors [J]. *IEEE Photon Technol Lett*, 2006, **18**(13): 1457-1459.

[13] TANI M, MATSUURA S, SAKAI K, *et al*. Multiple-frequency generation of sub-terahertz radiation by multimode LD excitation of photoconductive antenna [J]. *IEEE Microwave and Guided Wave Lett*, 1997, **7**(9): 282-284.

[14] BROWN E R, MCINTOSH K A, NICHOLS K B, *et al*. Photomixing up to 3.8 THz in low-temperature-grown GaAs [J]. *Appl Phys Lett*, 1995, **66**(3): 285-287.

[15] TANI M, MORIKAWA O, Matsuura S, *et al*. Generation of terahertz radiation by photomixing with dual- and multiple-mode lasers [J]. *Semicond Sci Technol*, 2005, **20**(7): S151-S163.

[16] GREGORY I S, TRIBE W R, COLE B E, *et al*. Resonant dipole antennas for continuous-wave terahertz photomixers [J]. *Appl Phys Lett*, 2004, **85**(9): 1622-1624.

[17] DUFFY S, VERGHESE S, MCINTOSH K, *et al*. Accurate modeling of dual dipole and slot elements used with photomixers for coherent terahertz output power [J]. *IEEE Trans Microwave Theory and Tech*, 2001, **49**(6): 1032-1038.

光电导天线辐射阻抗特性模拟分析

徐英[1]，陈海滨[1]，洪治[2]

(1 浙江大学 光及电磁波研究中心，杭州 310058)

(2 中国计量学院 太赫兹技术与应用研究所，杭州 310018)

摘　要：针对连续太赫兹光电导天线辐射功率较低的缺点，利用有限积分方法对三种常用的光电导天线，包括偶极天线、蝶形天线和螺旋天线，进行数值模拟并分析比较其辐射阻抗特性. 仿真结果表明，偶极天线的辐射阻抗与偶极长度、宽度、电极间隙以及传输线宽度有关，且在其谐振频率存在峰值阻抗，适用于特定频率的太赫兹波辐射. 蝶形天线和螺旋天线在所研究的太赫兹波段具有近似稳定的辐射阻抗，广泛应用于宽带领域. 对带有交叉电极的电极间隙进行计算，结果表明由交叉电极引入的附加电容降低了天线的高频阻抗.

关键词：太赫兹；光子混频；偶极天线；蝶形天线；螺旋天线

XU Ying　was born in 1982. Now she is pursuing her Ph. D. degree from Department of Opitcal Engineering, Zhejiang University. Her research interests focus on photoconductive antenna and continuous-wave terahertz system.

HONG Zhi　was born in 1964. He received the Ph. D. degree in optical engineering from Zhejiang University in 2001. Now he is a professor and director of Centre for Terahertz Research, China Jiliang University, and his main research interests focus on terahertz device, sensing, and imaging; lasers; quantum information processing.

光电导天线辐射阻抗特性模拟分析

作者： 徐英， 陈海滨， 洪治， XU Ying， CHEN Hai-bin， HONG Zhi

作者单位： 徐英,陈海滨,XU Ying,CHEN Hai-bin(浙江大学,光及电磁波研究中心,杭州,310058)， 洪治,HONG Zhi(中国计量学院,太赫兹技术与应用研究所,杭州,310018)

刊名： 光子学报 ISTIC PKU

英文刊名： ACTA PHOTONICA SINICA

年，卷(期)： 2010,39(2)

被引用次数： 3次

参考文献(17条)

1. GREGORY I S;TRIBE W R;BAKER C Continuous-wave terahertz system with a 60 dB dynamic range[外文期刊] 2005(20)

2. XI Zai-jun;XIAO Ti-qiao;ZHANG Zeng-yan Investigation on two-dimensional transmission imaging with terahertz wave by time domain spectroscopy[期刊论文]-Acta Photonica Sinica 2006(08)

3. MITTLEMAN D M;JACOBSEN R H;NUSS M C T-ray imaging[外文期刊] 1996(03)

4. NAKAJIMA S;HOSHINA H;Yamashita M Terahertz imaging diagnostics of cancer tissues with a chemometrics technique 2007(04)

5. JIA Wan-li;JI Wei-li;SHI Wei Two-dimensional Monte Carlo simulation of screening of the bias field in terahertz generation from semi_insulated GaAs photoconductors[期刊论文]-Acta Physica Sinica 2007(04)

6. LIU Ming-li;ZHANG Tong-yi;SUN Chuan-dong Characterization of high-power narrow-band terahertz radiation generation using large-aperture photoconductive antennas[期刊论文]-Acta Photonica Sinica 2007(10)

7. TANI M;GU P;HYODO M Generation of coherent terahertz radiation by photomixing of dual-mode lasers[外文期刊] 2000(04)

8. MATSUURA S;TANI M;SAKAI K Generation of coherent terahertz radiation by photomixing in dipole photoconductive antennas[外文期刊] 1997(03)

9. MCINTOSH K A;BROWN E R;NICHOLS K B Terahertz photomixing with diode lasers in low-temperature-grown GaAs 1995(26)

10. GREGORY I S;BAKER C;TRIBE W R Optimization of photomixers and antennas for continuous-wave terahertz emission[外文期刊] 2005(05)

11. BROWN E R A photoconductive model for superior GaAs THz photomixers[外文期刊] 1999(06)

12. SAEEDKIA D;SAFAVI-NAEINI S A comprehensive model for photomixing in ultrafast photoconductors[外文期刊] 2006(13)

13. TANI M;MATSUURA S;SAKAI K Multiple-frequency generation of sub-terahertz radiation by multimode LD excitation of photoconductive antenna[外文期刊] 1997(09)

14. BROWN E R;MCINTOSH K A;NICHOLS K B Photomixing up to 3.8 THz in low-temperature-grown GaAs[外文期刊] 1995(03)

15. TANI M;MORIKAWA O;Matsuura S Generation of terahertz radiation by photomixing with dual-and multiple-mode lasers[外文期刊] 2005(07)

如 何 学 习 天 线 设 计

天线设计理论晦涩高深，让许多工程师望而却步，然而实际工程或实际工作中在设计天线时却很少用到这些高深晦涩的理论。实际上，我们只需要懂得最基本的天线和射频基础知识，借助于 HFSS、CST 软件或者测试仪器就可以设计出工作性能良好的各类天线。

易迪拓培训(www.edatop.com)专注于微波射频和天线设计人才的培养，推出了一系列天线设计培训视频课程。我们的视频培训课程，化繁为简，直观易学，可以帮助您快速学习掌握天线设计的真谛，让天线设计不再难…

HFSS 天线设计培训课程套装

套装包含 6 门视频课程和 1 本图书，课程从基础讲起，内容由浅入深，理论介绍和实际操作讲解相结合，全面系统的讲解了 HFSS 天线设计的全过程。是国内最全面、最专业的 HFSS 天线设计课程，可以帮助你快速学习掌握如何使用 HFSS 软件进行天线设计，让天线设计不再难…

课程网址：http://www.edatop.com/peixun/hfss/122.html

CST 天线设计视频培训课程套装

套装包含 5 门视频培训课程，由经验丰富的专家授课，旨在帮助您从零开始，全面系统地学习掌握 CST 微波工作室的功能应用和使用 CST 微波工作室进行天线设计实际过程和具体操作。视频课程，边操作边讲解，直观易学；购买套装同时赠送 3 个月在线答疑，帮您解答学习中遇到的问题，让您学习无忧。

详情浏览：http://www.edatop.com/peixun/cst/127.html

13.56MHz NFC/RFID 线圈天线设计培训课程套装

套装包含 4 门视频培训课程，培训将 13.56MHz 线圈天线设计原理和仿真设计实践相结合，全面系统地讲解了 13.56MHz 线圈天线的工作原理、设计方法、设计考量以及使用 HFSS 和 CST 仿真分析线圈天线的具体操作，同时还介绍了 13.56MHz 线圈天线匹配电路的设计和调试。通过该套课程的学习，可以帮助您快速学习掌握 13.56MHz 线圈天线及其匹配电路的原理、设计和调试…

详情浏览：http://www.edatop.com/peixun/antenna/116.html

关于易迪拓培训：

易迪拓培训(www.edatop.com)由数名来自于研发第一线的资深工程师发起成立，一直致力和专注于微波、射频、天线设计研发人才的培养；后于 2006 年整合合并微波 EDA 网(www.mweda.com)，现已发展成为国内最大的微波射频和天线设计人才培养基地，成功推出多套微波射频以及天线设计经典培训课程和 ADS、HFSS 等专业软件使用培训课程，广受客户好评；并先后与人民邮电出版社、电子工业出版社合作出版了多本专业图书，帮助数万名工程师提升了专业技术能力。客户遍布中兴通讯、研通高频、埃威航电、国人通信等多家国内知名公司，以及台湾工业技术研究院、永业科技、全一电子等多家台湾地区企业。

我们的课程优势：

※ 成立于 2004 年，10 多年丰富的行业经验

※ 一直专注于微波射频和天线设计工程师的培养，更了解该行业对人才的要求

※ 视频课程、既能达到了现场培训的效果，又能免除您舟车劳顿的辛苦，学习工作两不误

※ 经验丰富的一线资深工程师主讲，结合实际工程案例，直观、实用、易学

联系我们：

※ 易迪拓培训官网：http://www.edatop.com

※ 微波 EDA 网：http://www.mweda.com

※ 官方淘宝店：http://shop36920890.taobao.com